Mapping Transition Metal-MN4 Macrocyclic Complex Catalysts Performance for the Critical Reactivity Descriptors

Available online at www.sciencedirect.com

ScienceDirect

Current Opinion in Electrochemistry

Review Article

Mapping transition metal-MN4 macrocyclic complex catalysts performance for the critical reactivity descriptors

José H. Zagal[1], Stefania Specchia[2] and Plamen Atanassov[3]

Abstract

There has been a significant progress toward the development of highly active and stable platinum group metal-free (PGM-free) electrocatalysts for the oxygen reduction reaction (ORR) in polymer electrolyte fuel cells, promising a low-cost replacement for Pt group electrocatalysts. However, the success of such developments depends on the implementation of PGM-free electrocatalysts that are not only highly active but importantly, they also exhibit long-term durability under polymer electrolyte fuel cell operating conditions. This manuscript is an overview of the current status of a specific, most advanced class of PGM-free electrocatalysts: transition metal−nitrogen−carbon ORR catalysts. We present an overview for the understanding of catalysts' performance descriptors for metal−nitrogen−carbon materials.

Addresses

[1] Laboratorio de Electrocatálisis y Electrónica Molecular, Departamento de Química de Los Materials, Universidad de Santiago de Chile, Ada. Bernardo O'higgins 3363, Santiago, 9170022, Chile

[2] Department of Applied Science & Technology, Politecnico di Torino, Corso Duca Degli Abruzzi 24, 10129, Torino, Italy

[3] Department of Chemical & Biomolecular Engineering and National Fuel Cell Research Center, University of California Irvine, CA, 92697, USA

Corresponding author: Zagal, Jos é H. (jose.zagal@usach.cl)Email address: stefania.specchia@polito.it (S. Specchia), plamen.atanassov@uci.edu (P. Atanassov)

Current Opinion in Electrochemistry 2021, **27:**100683

This review comes from a themed issue on **Innovative Methods in electrochemistry**

Edited by **Plamen Atanassov** and **Wolfgang Schuhmann**

For a complete overview see the Issue and the Editorial

Available online 2 January 2021

https://doi.org/10.1016/j.coelec.2020.100683

Keywords

Platinum group metal-free (PGM-Free) electrocatalysts, MN_4 transition metal−molecular catalysts, ORR electrocatalysts, Activity descriptors, Active site density (*SD*), Turn-over frequency (*TOF*).

Introduction

O_2/H_2 fuel cells were invented by Schönbein [1] and Grove [2] in 1839 and they are still not widely used. The 4-electron oxygen reduction reaction (ORR) is a very spontaneous reaction in H_2/O_2 fuel cells ($O_2 + 2H_2 \rightarrow 2H_2O$), but its kinetics are sluggish on most electrode surfaces because it involves several electron transfer steps and consequently several activation barriers [3]. The ORR at the cathode represents the bottleneck in fuel cell performance. The cathode requires the presence of expensive catalysts. Most active catalytic materials contain Pd or Pt-based catalysts (for alkaline and proton exchange membrane fuel cells, respectively) [4–8]. Catalysts containing very low amounts of highly dispersed Pt group metals have been developed, but they still contribute substantially to the cost of most fuel cells. For this reason, the search for less expensive catalysts using earth abundant elements has been active for five decades [9–15]. Earlier catalytic materials belonged to the MN_4 or MN_x class involving metal-phthalocyanines, metal-porphyrins, and molecules alike (refer Figure 1). These molecular catalysts are cheaper than Pt group metals and exhibit rather high activities when immobilized on graphitic and carbon surfaces, but most of them do not have long-term stability in fuel cells electrolytes, especially in acid [16–20]. However they have served as models to establish reactivity descriptors that essentially indicate that the metal centers need to have a rather positive M(III)/(II) redox potential (ideally close to the O_2/H_2O reversible potential) and moderate $M-O_2$ binding energies [21,22], essentially similar to those for Pt. On the other hand, their low stability has been improved by heat-treatment of intact MN_4 complexes or by pyrolysis using ingredients containing the necessary elements C, N, and a metal, generally Fe. Most MN_4 complexes have pyrrolic inner ligands, but pyrolyzed materials have pyridinic inner ligands, and they have been modeled recently using $Fe(phen)_2N_2$ chelates [23]. Many procedures have been reported to prepare these pyrolyzed materials involving heat treatments up to 1000 °C, and stability is linked to the method of preparation. Even though stability is crucial for practical applications, it is

an issue that has not been addressed with the same emphasis compared with that for achieving high activity [24–27]. Hence, it is important to develop unified stability–activity relationships as guidelines for the development of realistic catalysts for fuel cells.

Discussion

Recently, the attention has been focused on two reactivity descriptors, the active metal site density (SD $[mol_{site}\ cm^{-2}]$, or SD_{mass} $[site\ g_{cat}^{-1}]$, or SD_{vol} $[site\ cm^{-3}]$) and the catalytic turn-over frequency (TOF $[s^{-1}]$ or $[electron\ site^{-1}\ s^{-1}]$), that is the electrons transferred per active site per second [28]. Increasing the value of one, or both of these descriptors, predicts highly active electrocatalysts. The combination of TOF and SD, together with the Faraday constant F, the number of electrons involved in the reaction, n, and τ_{CL} the thickness of the catalyst layer, provide the kinetic activity of platinum group metal-free (PGM-free) catalysts at a specific potential [29,30]:

$$J_{kin}\ [A\ cm^{-2}] = n{\cdot}F\ [C\ mol^{-1}]$$

$$\cdot TOF\ [s^{-1}]{\cdot}SD\ [mol_{site}\ cm^{-2}]$$

or

$$J_{kin,mass}\ [A\ g^{-1}] = TOF\ [electron\ site^{-1}s^{-1}]$$

$$\cdot SD_{mass}\ [site\ g^{-1}]{\cdot}e\ [C\ electron^{-1}]$$

or

$$J_{kin,vol}\ [A\ cm^{-2}] = TOF\ [electron\ site^{-1}s^{-1}]$$

$$\cdot SD_{vol}\ [site\ cm^{-3}]{\cdot}e\ [C\ electron^{-1}]{\cdot}\tau_{CL}\ [cm]$$

The combination of TOF and SD can be considered as a rigorous comparison between catalysts [28]. TOF can be estimated in different ways and it is very important to know how they are estimated. A typical technique to measure both SD, or better the gravimetric site density SD_{mass} $[site\ g_{cat}^{-1}]$, and TOF, is represented by the *ex situ* low temperature (or cryo) CO chemisorption/desorption at −80 °C. CO rapidly and strongly adsorbs on oxygen-free Fe(II)-N_x sites [31]. Moreover, the amount of CO adsorbed is monotonic proportional to the ORR activity [32,33], i.e. one adsorbed CO molecule corresponds to one Fe(II)-N_x moiety at the surface of the catalyst. Thus, the measurement of the CO uptake, n_{CO}, allows calculating the SD_{mass}, which can be further used in combination with J_{kin} to calculate the TOF.

$$SD_{mass/CO}\ [site\ g_{cat}^{-1}] = n_{CO}[mol\ g_{cat}^{-1}]{\cdot}N_A[site\ mol^{-1}]$$

$$TOF_{CO}\ [s^{-1}] = \frac{J_{kin,mass}\ [A\ g_{cat}^{-1}]{\cdot}N_A[site\ mol^{-1}]}{F\ [C\ mol^{-1}]{\cdot}SD_{mass/CO}\ [site\ g_{cat}^{-1}]}$$

A strip protocol of cleaning the catalyst surface of oxygen, followed by a series of CO pulses to reach saturation of the active centers and the temperature program desorption allows a very precise measurement [32,33].

SD can also be estimated with an *in situ* electrochemical technique based on the adsorption of nitrite and electrostripping of NO through a 5-electron reaction on Fe(II)-N_x active sites, assuming that one NO molecule poisons one site. The determination of Q_{strip}, that is the excess coulometric charge associated with the stripping peak, together with the number of electrons necessary to reduce the nitrite ion, n_{strip}, and the specific surface area of the catalyst, S_{BET}, allows determining the SD. NO_2^- anions adsorption largely affects the ORR activity of the electrocatalyst, by poisoning the active sites. Thus, it is also possible to evaluate the TOF at a certain potential by measuring the kinetic mass current of the catalyst as the difference of the unpoisoned and poisoned kinetic mass current values, ΔJ_{kin} ($J_{kin,mass}^{unpoisoned} - J_{kin,mass}^{poisoned}$). This technique has been developed by the group of Kucernak et al. [29,30,34], it requires a series of subsequent steps of cleaning, poisoning, and stripping of the reaction products from the catalyst layer for the determination of Q_{strip} and ΔJ_{kin}.

$$SD_{mass/NO_2^-}\ [mol\ site\ g^{-1}] = \frac{Q_{strip}\ [C\ g^{-1}]}{n_{strip}{\cdot}F\ [C\ mol^{-1}]}$$

$$TOF_{NO_2^-}\ [s^{-1}] = \frac{\Delta J_{kin}\ [A\ g^{-1}]}{F\ [C\ mol^{-1}]{\cdot}SD_{mass/NO_2^-}\ [mol\ site\ g^{-1}]}$$

Double layer (DL) capacitance can be used to estimate the area of electrodes. For pyrolyzed catalysts, the wetted surface area can be estimated from Electrochemical Impedance Spectroscopy (EIS) measurements [35], but it is very dependent on the type of carbon or graphitic materials, graphitic edges, and presence of carbon functionalities [36]. Thus, DL capacitances can vary from as low as 4 μF cm^{-2} (defect-free basal plane graphite) to 60 μF cm^{-2} for more heterogeneous carbon/graphitic materials and in the average, most materials exhibit DL-capacitances around 20–25 μF cm^{-2} [36].

Figure 1

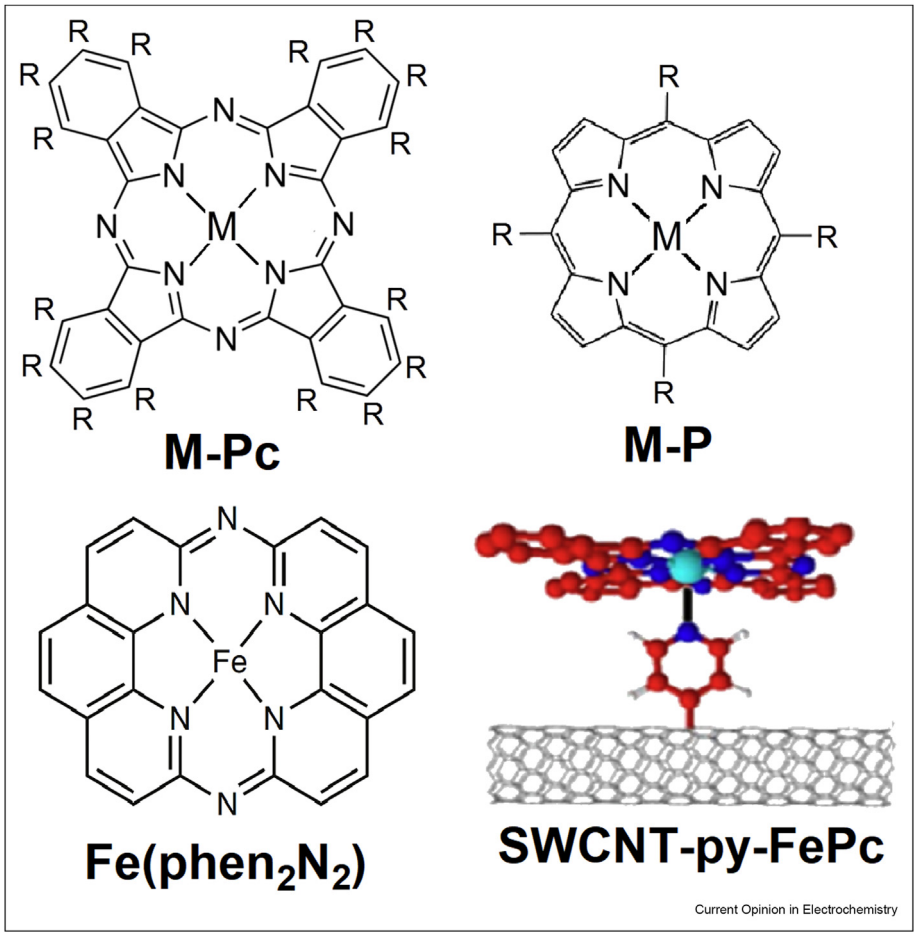

ORR molecular catalysts clockwise: metal-phthalocyanine, metal-porphyrin, Fe-(phenanthroline)$_2$N$_2$, and FePc anchored via a pyridine axial ligand to a single-walled carbon nanotube. ORR, oxygen reduction reaction.

It is important to know how *TOF* values are estimated. A correct *TOF* estimation should only consider the active sites available for the reaction. An overestimation will lead to lower *TOF* values. For example, a catalyst containing Fe as active sites, where Fe bulk is not effective for several reasons: oxygen has no access to those sites but they are considered in the *TOF* calculation. There could be another reason for those sites not be active: they are partially covered or occupied by adsorbed intermediates resulting from the reaction and another: some of those active sites are in the wrong oxidation state at the particular electrode potential. It is widely accepted that only M(II) is active.

This is illustrated in Figure 2a and shows a clear volcano correlation for several MN_4 molecular catalysts adsorbed on a smooth graphite surface. Hypothetically, it is assumed that all active sites are accessible to oxygen as the adsorbed MN_4 molecules are lying flat on the graphite surface, and there are no MN_4 molecules imbedded in the graphite. Those electrodes were made of graphite crystals, so porosity is very low or absent. NiPc shows low activity because the interaction between Ni and O_2 is too weak. The opposite is true for CrPc. The classical arguments for the low activity of CrPc would be that most active sites are occupied by strongly bound oxygen intermediates. However, the most important factor contributing to the low activity of CrPc is that its Cr(III)/(II) redox potential is too negative compared to the potential at which ORR currents are compared. Thus, most Cr sites are in the inactive state Cr(III). However, if the currents are divided by the fraction of sites $\theta_{M(II)}$ in the active state M(II) for all MN_4 catalysts, the volcano correlation becomes a linear correlation and the activity per active sites increases going from weak oxygen binding catalysts (right) to strong binding catalysts (left). The same happens if the *TOF* values are plotted versus the M—O_2

Figure 2

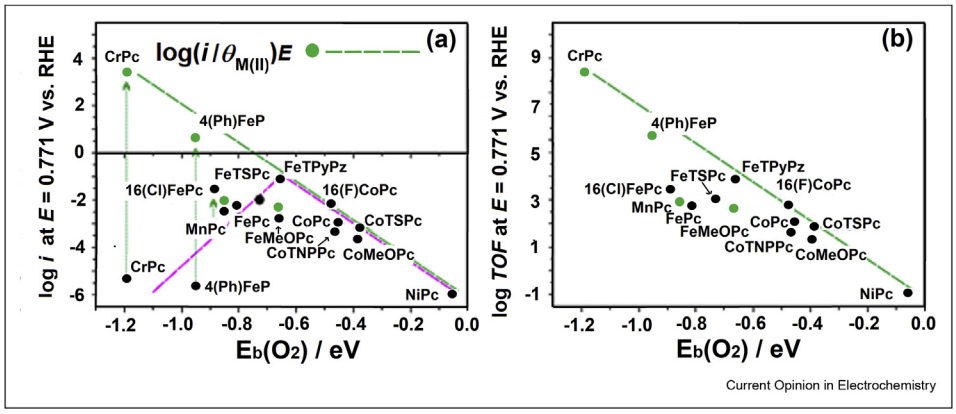

(a) Activity volcano and linear correlation for the catalytic activity toward ORR of a series of MN_4 complexes adsorbed on a smooth graphite surface versus M–O_2 binding energy. The linear correlation involves $\log(i/\theta_{M(II)})$, where $\theta_{M(II)}$ is fraction of Fe(II) sites estimated using the Nernst equation for adsorbed species. Data extracted from Zagal & Koper [50]. **(b)** Plot of $\log(TOF)_E$ for ORR versus the M–O_2 binding energy for several MN_4 molecular catalysts. Data taken from Figure 2a. ORR conditions for both graphs: 0.1 M NaOH and 25 °C. ORR, oxygen reduction reaction; TOF, turn-over frequency.

binding energy in Figure 2b, as $\log(i/\theta_{M(II)})_E$ values are directly proportional to *TOF* values but with the slight difference that for strongly binding catalysts $n = 4$ (O_2 reduction to OH^-) and for weak binding catalysts $n = 2$ (O_2 reduction to peroxide).

In Figure 2a CrPc shows very low activity but exhibits the highest *TOF* in Figure 2b. The best catalyst illustrated in Figure 2a is FePyPz that shows a *TOF* value almost 5 orders of magnitude lower than the poor CrPc catalyst. Yang et al. [37] reported a series of *TOF* values for the activity of FePc for ORR in 0.1 M KOH using several carbon substrates and they report values that vary in the range from 0.5 to 2.8 at $E = 0.868$ V vs RHE. However, these values are underestimated because that particular potential is the formal potential of the Fe(III)/(II) couple of FePc. At this potential $\theta_{Fe(II)} = 0.5$, consequently the *TOF* values are underestimated by a factor of 2. Therefore, errors can be introduced if the potential for comparing ORR currents is close to the potential of that redox couple. For pyrolyzed materials, $\theta_{M(II)}$ cannot be estimated easily as most of these materials exhibit no clear redox signals that can be attributed to the M(III)/(II) redox couple.

The two *in situ* and *ex situ* techniques mentioned before let the estimation of reactivity descriptors of PGM-free catalysts with a high degree of precision, and with comparable results. Usually, *TOF* values estimated from CO chemisorption result slightly lower that those calculated by nitrite stripping because of the overestimation of the related *SD*, or different way to calculate the kinetic current in the two methods [33]. Moreover, also the difference between gas-phase accessibility (CO chemisorption) and electrochemical accessibility (nitrite reactivity) plays a role in the different values obtained by measuring the *SD* by *in situ* or *ex situ* methods. In fact, the electrochemical surface can match rather well the gas-phase surface for Fe–N–C materials with low S_{BET} (specific surface area, that is, relatively low amount of micropores), although the two values can be quite different in the case of high S_{BET}, where the micropore area is prevalent [33]. However, Fe–N–C materials have modest intrinsic catalytic activity, lower than Pt, especially in acid, obliging increasing the catalytic loading at the cathode to compensate for the overall activity [28,38–40]. In addition, thicker catalytic layers represent a limitation in terms of mass transport resistance, electronic resistance, and proton resistance [38], not only at RDE level but especially at MEA (membrane electrode assembly) level, when testing polymer electrolyte fuel cells [40–42]. In fact, when working at high power density, thin electrodes are required to limit mass-transport–related voltage losses [43]. Thus, enhanced proton transport properties of the active site are essential for a high *TOF* in acid [44]. Just as an example, Pt-based catalysts can easily reach *TOF* values ranging between 10 and 42 e^- $site^{-1}$ s^{-1} at reported conditions [28,43], whereas Fe–N–C materials are at much lower order of magnitude, not overcoming 2 e^- $site^{-1}$ s^{-1} at reported conditions [33,45].

Catalysts based on N_4-metal chelates

Different groups have investigated MN_4 macrocyclic complexes not subjected to any heat treatment. They provide simple models to identify some reactivity descriptors because active sites are clearly identified,

especially the metal centers in the MN_4 moiety [21] as showing well-defined CV redox peaks attributed to metal-centered redox processes. The charge under those reversible peaks allows the accurate determination of the amount or electroactive catalysts present as SD $[mol_{site}\ cm^{-2}]$. Most reports agree that they lack the long-time stability/durability required for fuel-cell performance, especially in acid. However, Cao et al. [46] reported that FePc can exhibit higher activity than Pt/C in alkaline media and a stability higher than 1000 cycles, when anchored on carbon nanotubes via a pyridine axial ligand (FePc-Py-SWCNT) (refer Figure 1). Yang et al. [37] have studied FePc as well and directly deposited on different nanocarbons. The activity depends strongly on the type of carbon substrate used. Figure 3a illustrates the *TOF* values for FePc on different carbon supports and the highest *TOF* value is observed when C450, a 3D nanoporous C with macropores of 450 nm, is used [37]. The low stability of FePc-based catalysts having high *TOF* values could be due to the fact that highly reactive sites for ORR can also be highly reactive to other species and/or intermediates such as peroxide and OH radicals that are generated faster than less active catalysts attacking those sites, besides carbon corrosion [35]. Similar mechanisms have been described for pyrolyzed metal−nitrogen−carbon catalysts [33,46].

Yang et al. [37] calculated these *TOF* values according to

$$TOF\ \left[s^{-1}\right] = \frac{i\left[A\ cm^{-2}\right]}{4{\cdot}Q_{Fe,active}\left[C\ cm^{-2}\right]}$$

where i is the current at 0.868 V_{RHE} and $Q_{Fe,active}$ represents the amount of electrochemically active centered Fe ion, estimated from the area of the Fe(III)/(II) redox peak determined by cyclic voltammetry under N_2-saturated 0.1 KOH. $Q_{Fe,active}$ depends on the morphology of the carbon support (specific surface area, pore structure, and roughness of the surface of the carbon), which affects somehow the amount of FePc deposited on the support itself at equal deposition procedures [37].

As explained before, those *TOF* values in Fig. 3 are probably underestimated because the number of Fe(II) active sites could be lower than the total sites N (mol cm^{-2}). In fact, at that particular potential, a fraction of the sites are in the oxidation state Fe(III) as 0.868 V_{RHE} is too close to the Fe(III)/(II) formal potential of the catalyst. A rough estimation using a formal potential of 0.868 V_{RHE} using the Nernst equation (estimated from the peak of CV curves reported, which coincides with the potential used for comparing activities) indicates that only ca. 50% of the catalyst is active as Fe(II). Fe(III) in alkaline media does not catalyze ORR as those sites are strongly binding OH^- ions [21]. However, the order of activity totally changes after a chronoamperometry at 0.868 V_{RHE}, showing that the most durable catalyst (that is the one that lasted longer before reaching the 50% current loss) was the one with the lowest *TOF* value (FePc/KBC) [37]. Interestingly, the results denote a shorter durability with *TOF* increasing. This effect can be explained considering that a low *TOF* value implies a slower formation of reaction intermediates during ORR, such as HO_2^-, which can partially hinder the active site. Thus, degradation is limited compared with catalysts with higher *TOF* values.

Cao et al. [46] did not provide any *TOF*, *SD* values, or CV profiles that could allow the estimation of *Q*. The

Figure 3

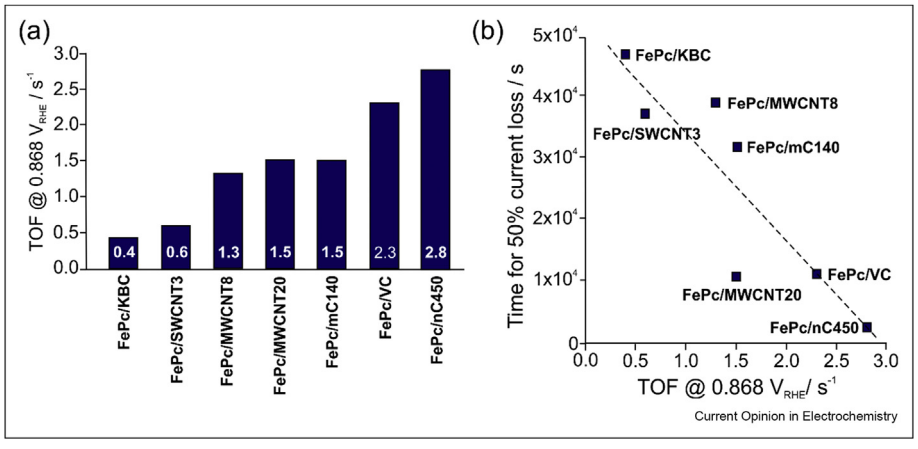

(a) Turn-over frequency (*TOF*) of catalysts containing FePc attached to the surface of different carbon supports (KBC, Ketjen Black carbon; VC, Vulcan carbon; WMCNT8, multi-wall carbon nanotube with diameter 8−15 nm; WMCNT20, multi-wall carbon nanotube with diameter 20 nm; SMCNT3, single-wall carbon nanotube with diameter 3−5 nm; nC450, 3D nanoporous carbon with macropores 450 nm; mC140, mesoporous carbon with macropores 140 nm). **(b)** Time for 50% current loss as a function of *TOF* at 0.868 V vs RHE. Data from Yang et al. [37].

enhancement of the activity of FePc when using a pyridine back-ligand seem to be associated to the electron-withdrawing effect of pyridine that would shift the Fe(III)/(II) redox potential in the positive direction and push the catalyst up towards the top of the volcano correlation of $(\log i)_E$ versus the $E\underline{o}'_{Fe(III)/(II)}$ of the catalyst [21]. The beneficial effect of an electron-withdrawing axial ligand on Fe phthalocyanines has been demonstrated using several FePcs attached to carbon nanotubes [48,49] substrates and gold (111) [50]. These axial ligands seem to mimic the action of similar ligands in enhancing the catalytic activity for ORR of cytochrome-c in the respiratory chain of aerobic life [47,51].

C–N materials show ORR activity even in the absence of any transition metal. Chakraborty et al. [52] have proposed a method for evaluating the active SD of metal-free nitrogen-doped carbon using catechol as an adsorbate. These catechol provide well-defined redox peaks that facilitate an indirect estimation of the mass-specific active SD (SD_{mass}) evaluated from the electrical charge involved in these redox processes according to:

$$SD_{mass}\left[\text{active site}\,g^{-1}\right] = \frac{\text{Integrated CV area}\,[AV]\cdot N_A\left[sitemol^{-1}\right]}{n\cdot scanrate[Vs^{-1}]\cdot F\left[Cmol^{-1}\right]\cdot m[g]}$$

where N_A is the Avogadro number, n the number of electrons, m is the catalyst's mass. The rest of terms have the usual meaning. The electrochemical surface area can be estimated according to (using the normalizing factor of 611 μC cm^{-2} as charge of unit surface area on graphite [53]):

$$ESA\left[cm^2g^{-1}\right] = \frac{Cat_{ads}charge[C]}{2\cdot m[g]\cdot 611\left[\mu C\ cm^{-2}\right]}$$

Chakraborty et al. [52] double checked their electrochemical surface area estimation using the equation mentioned previously using the BET-specific surface area (S_{BET}) and multiplied it by the total pyridinic nitrogen percentage, as reported by Guo et al. [53] and found comparable results suggesting the accuracy of the equation aforementioned. This is important for intact and pyrolyzed catalysts as nonmetallic sites can contribute to the catalytic process.

Conclusions

Most intact MN_4 complexes do not exhibit long-term stabilities that can be compatible with fuel performance. This is less critical in alkaline media, and there are some reports that might promise some success in this sense if the FeN_4 complexes are attached to carbon nanotubes directly or linked via pyridinic axial ligands.

The combination of *TOF* and *SD* can be considered as a rigorous comparison between catalysts [28]. There are different ways of estimating *TOF* values and the values obtained depend on the method used. This is relevant to both intact and pyrolyzed materials. *SD* should consider only active sites that are available for ORR. Bulk sites do not count. When using *TOF* values, special care needs to be taken in estimating the amount of M(II) active sites present under operating conditions (electrode potential) because some complexes could exhibit M(III)/(II) redox potentials close to the operating potential.

Finally, it has been suggested recently that intact complexes, which possess pyrrolic N inner nitrogens are not representative of real active sites present in MN_x pyrolyzed catalysts, which predominantly pyridinic N inner ligands. In this case, complex having phenanthroline inner ligands can serve as better models for future studies.

Credit author statement

The authors contribute equally to the work by discussing and writing the manuscript, drawing the figures, along with approving its final version.

Declaration of competing interest

The authors declare that they have no known competing financial interests or personal relationships that could have appeared to influence the work reported in this paper.

Acknowledgements

J.H.Z. acknowledges the funding from Anillo Project ACT 192175 Chile and Fondecyt Project 1181037. S.S. and P.A. acknowledge the funding provided by the Staff Mobility for Training & Teaching between Programme and Partner Countries within the Program Erasmus+/KA1 Higher Education action KA107 (International Credit Mobility, years 2017 and 2018) for the reciprocal visits @ UCI (in 2019) and POLITO (in 2020), respectively.

References

1. Schönbein CF: **On the voltaic polrization of certain solid and fluid substances**. *London Edinburgh Dublin Philos Mag J Sci* 1839:43–45.

2. Grove WR: **On voltaic series and the combination of gases by platinum**. *London Edinburgh Philos Mag J Sci* 1839, **3**:127–130.

3. Ramaswamy N, Mukerjee S: **Fundamental mechanistic understanding of electrocatalysis of oxygen reduction on Pt and non-Pt surfaces: acid versus alkaline media**. *Adv Phys Chem* 2012, **2012**:1–17, https://doi.org/10.1155/2012/491604.
An outstanding paper explaining complex electrochemical reactions such as ORR involving multi-electron transfer, depending on the nature of the electrode surface. The main differences between ORR in acid and alkaline media are clearly elucidated.

4. Shao M: **Palladium-based electrocatalysts for hydrogen oxidation and oxygen reduction reactions**. *J Power Sources* 2011, **196**:2433–2444, https://doi.org/10.1016/j.jpowsour.2010.10.093.

5. Čolić V, Bandarenka AS: **Pt alloy electrocatalysts for the oxygen reduction reaction: from model surfaces to nanostructured systems**. *ACS Catal* 2016, **6**:5378–5385, https://doi.org/10.1021/acscatal.6b00997.

6. Greeley J, Stephens IEL, Bondarenko AS, Johansson TP, Hansen HA, Jaramillo TF, Rossmeisl J, Chorkendorff I, Nørskov JK: **NoAlloys of platinum and early transition metals as oxygen reduction electrocatalysts**. *Nat Chem* 2009, **1**: 552–556, https://doi.org/10.1038/nchem.367.

7. Asset T, Chattot R, Fontana M, Mercier-Guyon B, Job N, Dubau L, Maillard F: **A review on recent developments and prospects for the oxygen reduction reaction on hollow Pt-alloy nanoparticles**. *ChemPhysChem* 2018, **19**:1552–1567, https://doi.org/10.1002/cphc.201800153.

8. Oezaslan M, Hasché F, Strasser P: **Pt-based core-shell catalyst architectures for oxygen fuel cell electrodes**. *J Phys Chem Lett* 2013, **4**:3273–3291, https://doi.org/10.1021/jz4014135.

9. Jasinski R: **A new fuel cell cathode catalyst**. *Nature* 1964, **201**: 1212–1213, https://doi.org/10.1038/2011212a0.
A pioneering paper being part of the history of the development of PGM-free catalysts based on Fe–N–C materials for ORR: metal phthalocyanines used as cathode catalysts in fuel cells.

10. Shao M, Chang Q, Dodelet J-P, Chenitz R: **Recent advances in electrocatalysts for oxygen reduction reaction**. *Chem Rev* 2016, **116**:3594–3657, https://doi.org/10.1021/acs.chemrev.5b00462.

11. Tammeveski K, Zagal JH: **Electrocatalytic oxygen reduction on transition metal macrocyclic complexes for anion exchange membrane fuel cell application**. *Curr Opin Electrochem* 2018, **9**: 207–213, https://doi.org/10.1016/j.coelec.2018.04.001.

12. Osmieri L, Pezzolato L, Specchia S: **Recent trends on the application of PGM-free catalysts at the cathode of anion exchange membrane fuel cells**. *Curr Opin Electrochem* 2018, **9**: 240–256, https://doi.org/10.1016/j.coelec.2018.05.011.

13. Serov A, Shum AD, Xiao X, De Andrade V, Artyushkova K, Zenyuk IV, Atanassov P: **Nano-structured platinum group metal-free catalysts and their integration in fuel cell electrode architectures**. *Appl Catal B Environ* 2018, **237**:1139–1147, https://doi.org/10.1016/j.apcatb.2017.08.067.

14. Osmieri L: **Transition metal–nitrogen–carbon (M–N–C) catalysts for oxygen reduction reaction. Insights on synthesis and performance in polymer electrolyte fuel cells**. *Chem-Engineering* 2019, **3**:16, https://doi.org/10.3390/chemengineering3010016.

15. Monteverde Videla AHA, Osmieri L, Specchia S: **Non-noble metal (NNM) catalysts for fuel cells: tuning the activity by a rational step-by-step single variable evolution**. In *Electrochem. N4 Macrocycl. Met. Complexes Vol. 1 Energy*. Edited by Zagal JH, Fethi B. 2nd ed., Switzerland: Springer Nature; 2016:69–102, https://doi.org/10.1007/978-3-319-31172-2_3.

16. Workman MJ, Serov A, Tsui LK, Atanassov P, Artyushkova K: **Fe-N-C catalyst graphitic layer structure and fuel cell performance**. *ACS Energy Lett* 2017, **2**:1489–1493, https://doi.org/10.1021/acsenergylett.7b00391.

17. Matanovic I, Artyushkova K, Atanassov P: **Understanding PGM-free catalysts by linking density functional theory calculations and structural analysis: perspectives and challenges**. *Curr Opin Electrochem* 2018, **9**:137–144, https://doi.org/10.1016/j.coelec.2018.03.009.

18. Thompson ST, Wilson AR, Zelenay P, Myers DJ, More KL, Neyerlin KC, Papageorgopoulos D: **ElectroCat: DOE's approach to PGM-free catalyst and electrode R&D**. *Solid State Ionics* 2018, **319**:68–76, https://doi.org/10.1016/j.ssi.2018.01.030.

19. Wang W, Jia Q, Mukerjee S, Chen S: **Recent insights into the oxygen-reduction electrocatalysis of Fe/N/C materials**. *ACS Catal* 2019, **9**:10126–10141, https://doi.org/10.1021/acscatal.9b02583.

20. Zagal JH: **Electrochemistry, past, present, and future: energy conversion, sensors, and beyond**. *J Solid State Electrochem* 2020, **24**:2195–2197, https://doi.org/10.1007/s10008-020-04707-x.

21. Zagal JH, Koper MTM: **Reactivity descriptors for the activity of molecular MN4 catalysts for the oxygen reduction reaction**. *Angew Chem Int Ed* 2016, **55**:14510–14521, https://doi.org/10.1002/anie.201604311.
An outstanding review paper providing a view on reactivity descriptors of highly active PGM-free catalysts.

22. Govan J, Abarca G, Aliaga C, Sanhueza B, Orellana W, Cárdenas-Jirón G, Zagal JH, Tasca F: **Influence of cyano substituents on the electron density and catalytic activity towards the oxygen reduction reaction for iron phthalocyanine. The case for Fe(II) 2,3,9,10,16,17,23,24-octa(cyano) phthalocyanine**. *Electrochem Commun* 2020, **118**:106784, https://doi.org/10.1016/j.elecom.2020.106784.

23. Marshall-Roth T, Libretto NJ, Wrobel AT, Anderton K, Ricke ND, Van Voorhis T, Miller JT, Surendranath Y: **A pyridinic Fe-N_4 macrocycle effectively models the active sites in Fe/N-doped carbon electrocatalysts**. *Chem Rxiv* 2019:1–21, https://doi.org/10.26434/CHEMRXIV.10008545.V1.
An outstanding paper elucidating that iron active sites in this class of materials exist in an Fe–N_4 pyridinic ligation environment. Electrochemical data indicate that the iron center in ($phen_2N_2$)Fe displays excellent selectivity to 4-electron ORR This study provides a rich platform for constructing high-performance Fe-based oxygen reduction catalysts.

24. Masa J, Andronescu C, Schuhmann W: **Electrocatalysis as the nexus for sustainable renewable energy. The Gordian knot of activity, stability, and selectivity**. *Angew Chem Int Ed* 2020, https://doi.org/10.1002/anie.202007672. anie.202007672.
An outstanding review paper showing how difficult, and sometimes controversial, is the research on PGM-free electrocatalysts. Understanding of reaction pathways and advanced in operando characterizations should become integral tools in material design.

25. Martinez U, Komini Babu S, Holby EF, Zelenay P: **Durability challenges and perspective in the development of PGM-free electrocatalysts for the oxygen reduction reaction**. *Curr Opin Electrochem* 2018, **9**:224–232, https://doi.org/10.1016/j.coelec.2018.04.010.

26. Chen L, Liu X, Zheng L, Li Y, Guo X, Wan X, Liu Q, Shang J, Shui J: **Insights into the role of active site density in the fuel cell performance of Co-N-C catalysts**. *Appl Catal B Environ* 2019, **256**:117849, https://doi.org/10.1016/j.apcatb.2019.117849.
An interesting paper showing how varying the synthesis can be helpful in modyfing the morphology of a catalyst to increase its activity, in particular the turnover frequency and the site density.

27. Martinaiou I, Monteverde Videla AHA, Weidler N, Kübler M, Wallace WDZ, Paul S, Wagner S, Shahraei A, Stark RW, Specchia S, Kramm UI: **Activity and degradation study of an Fe-N-C catalyst for ORR in direct methanol fuel cell (DMFC)**. *Appl Catal B Environ* 2020, **262**:118217, https://doi.org/10.1016/j.apcatb.2019.118217.

28. Gasteiger HA, Kocha SS, Sompalli B, Wagner FT: **Activity benchmarks and requirements for Pt, Pt-alloy, and non-Pt oxygen reduction catalysts for PEMFCs**. *Appl Catal B Environ* 2005, **56**:9–35, https://doi.org/10.1016/j.apcatb.2004.06.021.

29. Malko D, Lopes T, Ticianelli EA, Kucernak A: **A catalyst layer optimisation approach using electrochemical impedance spectroscopy for PEM fuel cells operated with pyrolysed transition metal-N-C catalysts**. *J Power Sources* 2016, **323**: 189–200, https://doi.org/10.1016/j.jpowsour.2016.05.035.

30. Malko D, Kucernak A, Lopes T: **In situ electrochemical quantification of active sites in Fe-N/C non-precious metal catalysts**. *Nat Commun* 2016, **7**:1–7, https://doi.org/10.1038/ncomms13285.
An interesting paper explaining in detail the procedure for the determinationof the site density and turnover frequency using the reversible nitrite adsorption followed by reductive stripping.

31. Birry L, Zagal JH, Dodelet J-P: **Does CO poison Fe-based catalysts for ORR?** *Electrochem Commun* 2010, **12**:628–631, https://doi.org/10.1016/j.elecom.2010.02.016.

32. Sahraie NR, Kramm UI, Steinberg J, Zhang Y, Thomas A, Reier T, Paraknowitsch JP, Strasser P: **Quantifying the density and utilization of active sites in non-precious metal oxygen electroreduction catalysts**. *Nat Commun* 2015, **6**:1–9, https://doi.org/10.1038/ncomms9618.

33. Primbs M, Sun Y, Roy A, Malko D, Mehmood A, Sougrati M-T, Blanchard P-Y, Granozzi G, Kosmala T, Daniel G, Atanassov P,

Sharman J, Durante C, Kucernak A, Jones DJ, Jaouen F, Strasser P: **Establishing reactivity descriptors for platinum group metal (PGM)-free Fe-N-C catalysts for PEM fuel cells**. *Energy Environ Sci* 2020, https://doi.org/10.1039/d0ee01013h.
An outstanding paper reporting a comprehensive analysis of the oxygen reduction activity of four well-known Fe−N−C-catalysts from different laboratories. Maps of site density versus to run over frequency are proposed as a rational tool for the engineering development of PGM-free catalysts.

34. Malko D, Kucernak A, Lopes T: **Performance of Fe−N/C oxygen reduction electrocatalysts toward NO_2^-, NO, and NH2OH electroreduction: from fundamental insights into the active center to a new method for environmental nitrite destruction**. *J Am Chem Soc* 2016, **138**:16056−16068, https://doi.org/10.1021/jacs.6b09622.

35. Chakraborty A, Bera B, Priyadarshani D, Leuaa P, Choudhury D, Neergat M: **Electrochemical estimation of active site density on a metal-free carbon-based catalyst**. *RSC Adv* 2019, **9**: 466−475, https://doi.org/10.1039/C8RA08906J.

36. Kinoshita K: *Carbon materials: carbon—electrochemical and physicochemical properties*. 1st ed. Wiley-Interscience; 1988.

37. Yang J, Tao J, Isomura T, Yanagi H, Moriguchi I, Nakashima N: **A comparative study of iron phthalocyanine electrocatalysts supported on different nanocarbons for oxygen reduction reaction**. *Carbon NY* 2019, **145**:565−571, https://doi.org/10.1016/j.carbon.2019.01.022.

38. Jaouen F, Jones D, Coutard N, Artero V, Strasser P, Kucernak A: **Toward platinum group metal-free catalysts for hydrogen/air proton-exchange membrane fuel cells**. *Johns Matthey Technol Rev* 2018, **62**:231−255, https://doi.org/10.1595/205651318X696828.
An interesting review paper showing the status, concepts and challenges toward PGM-free catalysts for oxygen reduction reaction. With a specific focus on the interplay between volumetric activity, thickness and transport proerties determining the cathode performance.

39. Osmieri L, Monteverde Videla AHA, Ocón P, Specchia S: **Kinetics of oxygen electroreduction on Me-N-C (Me = Fe, Co, Cu) catalysts in acidic medium: insights on the effect of the transition metal**. *J Phys Chem C* 2017, **121**:17796−17817, https://doi.org/10.1021/acs.jpcc.7b02455.
An interesting paper showing the influence of different transition metals on the kinetics of ORR in acidic medium.

40. Osmieri L, Wang G, Cetinbas FC, Khandavalli S, Park J, Medina S, Mauger SA, Ulsh M, Pylypenko S, Myers DJ, Neyerlin KC: **Utilizing ink composition to tune bulk-electrode gas transport, performance, and operational robustness for a Fe−N−C catalyst in polymer electrolyte fuel cell**. *Nano Energy* 2020, **75**:104943, https://doi.org/10.1016/j.nanoen.2020.104943.
An outstanding paper demonstrating how electrode optimization and electrode design can improve proton conductivity and bulk-electrode gas transport properties. These activities are critical for the improvement of PGM-free electrodes performance as much as the increase in catalyst activity and stability.

41. Osmieri L, Mauger S, Ulsh M, Neyerlin KC, Bender G: **Use of a segmented cell for the combinatorial development of platinum group metal-free electrodes for polymer electrolyte fuel cells**. *J Power Sources* 2020, **452**, https://doi.org/10.1016/j.jpowsour.2020.227829.

42. Wang G, Osmieri L, Star AG, Pfeilsticker J, Neyerlin KC: **Elucidating the role of ionomer in the performance of platinum group metal-free catalyst layer via in situ electrochemical diagnostics**. *J Electrochem Soc* 2020, **167**, 044519, https://doi.org/10.1149/1945-7111/ab7aa1.

43. Zelenay P, Myers DJ: *ElectroCat (Electrocatalysis Consortium)*. 2020. https://www.hydrogen.energy.gov/pdfs/review20/fc160_myers_zelenay_2020_o.pdf.

44. Park JY, Kwak DH, Ma KB, Han SB, Chai GS, Kim SK, Peck DH, Kim CS, Kucernak A, Park KW: **Enhanced oxygen reduction reaction of Pt deposited Fe/N-doped bimodal porous carbon nanostructure catalysts**. *J Catal* 2018, **359**:46−54, https://doi.org/10.1016/j.jcat.2017.12.033.

45. Luo F, Choi CH, Primbs MJM, Ju W, Li S, Leonard ND, Thomas A, Jaouen F, Strasser P: **Accurate evaluation of active-site density (SD) and turnover frequency (TOF) of PGM-free metal-nitrogen-doped carbon (MNC) electrocatalysts using CO cryo adsorption**. *ACS Catal* 2019, **9**:4841−4852, https://doi.org/10.1021/acscatal.9b00588.

46. Cao R, Thapa R, Kim H, Xu X, Kim MG, Li Q, Park N, Liu M, Cho J: **Promotion of oxygen reduction by a bio-inspired tethered iron phthalocyanine carbon nanotube-based catalyst**. *Nat Commun* 2013, **4**:1−7, https://doi.org/10.1038/ncomms3076.

47. Cao R, Thapa R, Kim H, Xu X, Kim MG, Li Q, Park N, Liu M, Cho J: **Promotion of oxygen reduction by a bio-inspired tethered iron phthalocyanine carbon nanotube-based catalyst**. *Nat Commun* 2013, **4**:1−7, https://doi.org/10.1038/ncomms3076.

48. Venegas R, Recio FJ, Riquelme J, Neira K, Marco JF, Ponce I, Zagal JH, Tasca F: **Biomimetic reduction of O_2 in an acid medium on iron phthalocyanines axially coordinated to pyridine anchored on carbon nanotubes**. *J Mater Chem A* 2017, **5**: 12054−12059, https://doi.org/10.1039/c7ta02381b.

49. Zagal JH, Kruusenberg I, Tammeveski K, Recio KMJ, Venegas R: **Oxygen reduction on carbon-supported metallophthalocyanines and metalloporphyrins**. *Encycl Interfacial Chem* 2018:812−819, https://doi.org/10.1016/B978-0-12-409547-2.13572-3.

50. Pizarro A, Abarca G, Gutiérrez-Cerón C, Cortés-Arriagada D, Bernardi F, Berrios C, Silva JF, Rezende MC, Zagal JH, Onate R, Ponce I: **Building pyridinium molecular wires as axial ligands for tuning the electrocatalytic activity of iron phthalocyanines for the oxygen reduction reaction**. *ACS Catal* 2018, **8**: 8406−8419, https://doi.org/10.1021/acscatal.8b01479.

51. Boulatov R: **Billion-year-old oxygen cathode that actually works: respiratory oxygen reduction and its biomimetic analogs**. In *N_4-Macrocyclic Met. Complexes*. Edited by Zagal JH, Bedioui F, Dodelet J-P. 1st ed., New York: Springer-Verlag New York; 2006:814, https://doi.org/10.1007/978-0-387-28430-9_1.

52. Chakraborty A, Devivaraprasad R, Bera B, Neergat M: **Electrochemical estimation of the active site density on metal-free nitrogen-doped carbon using catechol as an adsorbate**. *Phys Chem Chem Phys* 2017, **19**:25414−25422, https://doi.org/10.1039/c7cp04285j.

53. Guo D, Shibuya R, Akiba C, Saji S, Kondo T, Nakamura J: **Active sites of nitrogen-doped carbon materials for oxygen reduction reaction clarified using model catalysts**. *Science (80-)* 2016, **351**:361−365, https://doi.org/10.1126/science.aad0832.